

# A Backwards Error Analysis Approach for Simulation and Control of Nonsmooth Mechanical Systems

David Pekarek and Todd D. Murphey

**Abstract**—This paper presents an original structured integration scheme for Lagrangian systems undergoing elastic impacts due to unilateral constraints. In deriving the method, a backwards error analysis approach establishes a discrete time conservation law for impacts using the notion of a modified system Hamiltonian. Shortcomings of existing simulation methods that do not use this conservation law are demonstrated both analytically and in simulation. Relative to these methods, our scheme provides advantages in terms of discrete time energy behavior, accuracy of trajectories, and consistent order of accuracy of the method.

## I. INTRODUCTION

There are a variety of mechanical systems that, in their interaction with other systems and their environment, exhibit behaviors that involve collisions and contact between surfaces. These behaviors induce dynamics in which body velocities, accelerations, and forces may be nonsmooth or even discontinuous. Much of the modern treatment of modeling these systems has involved generalizing Newton's law to include measure valued forces according to the theory of measure differential inclusions [4]. An alternative approach for modeling is to extend variational principles from smooth classical mechanics to include nonsmooth trajectories [19], [11]. This technique, which is followed in this paper, can provide extensive insight into the nonsmooth mechanics and associated conservation laws, but is oft restricted by difficult or lacking existence and uniqueness results for solutions.

Discrete time representations of nonsmooth mechanics enable computational tools for simulation and control design. For the aforementioned mechanical models derived with variational principles, a natural discretization scheme is the use of discrete mechanics and variational integrator (VI) theory [14], [7]. For simulating smooth mechanical systems, a VI's equations of motion are derived from a discretized variational principle and provide exact discrete momentum conservation, exact discrete symplectic form conservation, and stable discrete time energy behavior. To perform control design for mechanical systems, every VI naturally extends to a direct method for optimal control via the method of Discrete Mechanics and Optimal Control (DMOC) [10]. DMOC recasts a standard continuous time optimal control problem as a finite dimensional nonlinearly constrained optimization which is solvable with sequential quadratic programming.

D. Pekarek is a Postdoctoral Research Fellow in Mechanical Engineering at Northwestern University, Evanston, IL, USA [d-pekarek@northwestern.edu](mailto:d-pekarek@northwestern.edu)

T. D. Murphey is an Assistant Professor in Mechanical Engineering at the McCormick School of Engineering at Northwestern University, Evanston, IL, USA [t-murphey@northwestern.edu](mailto:t-murphey@northwestern.edu)

The DMOC method has already been successfully applied in optimal gait searches for bipedal robot models [18], [17], which represent a specific class of dissipative nonsmooth mechanical systems.

In this work we present and compare discrete time representations of conservative nonsmooth mechanical systems. There is an existing VI for this class of systems [5] that maintains the two aforementioned exact conservation laws (momentum, symplecticity). However, while simulating with this scheme we have found unstable energy behavior through collisions, even with relatively simple example systems. We propose a new method that is based on an existing backwards error analysis for smooth VIs. Our method is a variant of that in [3], and thus focuses on stabilizing energy behavior in the presence of impacts. Relative to the existing VI of [5], our method is not fully symplectic and requires a higher computational expense per impact, but offers greater accuracy, more consistent order of accuracy, and expectedly more stable discrete energy behavior. As a result of these desirable properties, our method will yield computational savings when performing nonsmooth system simulation and control design to a specified level of accuracy.

The structure of this paper is as follows. Section II presents a continuous time model of elastic impacts in the context of Lagrangian mechanics, Hamiltonian mechanics, and hybrid automata. Section III provides definitions and analytical analysis of three methods (two existing and our one original) for the structured integration of elastic impacts. Section IV provides a comparison of the integration methods in simulation, demonstrating the varied advantages of our original method.

## II. MECHANICAL SYSTEMS SUBJECT TO ELASTIC IMPACTS

In this section, we will review continuous time nonsmooth mechanics, in both the Lagrangian and Hamiltonian settings, for a system undergoing elastic impacts due to the presence of a unilateral constraint. For a specific class of systems, we will demonstrate that these impact mechanics fit the model of a hybrid automaton, defined with guard conditions and explicit reset maps. These continuous time descriptions of impact will aid in deriving and contrasting discrete time simulation methods in the coming sections.

### A. Variational Lagrangian Impact Mechanics

To begin our discussion of nonsmooth mechanics, we establish the following system model for the remainder of the paper. Consider a mechanical system with configuration

space  $Q$  (assumed to be an  $n$ -dimensional smooth manifold with local coordinates  $q$ ) and a Lagrangian  $L : TQ \rightarrow \mathbb{R}$ . We will treat this system in the presence of a one-dimensional, holonomic, unilateral constraint defined by a smooth function  $\phi : Q \rightarrow \mathbb{R}$  such that the feasible space of the system is  $C = \{q \in Q \mid \phi(q) \geq 0\}$ . We assume  $C$  is a submanifold with boundary in  $Q$ . Furthermore, we assume that 0 is a regular point of  $\phi$  such that the boundary of  $C$ ,  $\partial C = \phi^{-1}(0)$ , is a submanifold of codimension 1 in  $Q$ . Physically,  $\partial C$  is the set of contact configurations.

To derive the nonsmooth impact mechanics of the Lagrangian system above, we will follow the variational approaches of [11], [5]. Therein, it is shown that system trajectories satisfy a space-time formulation of Hamilton's principle of least action. For a trajectory  $q(t)$  that experiences a single impact at time  $t_i$  on the time interval  $[0, T]$ , this principle appears in its common form

$$\delta \int_0^T L(q(t), \dot{q}(t)) dt = 0, \quad (1)$$

but in addition to the typical variations  $\delta q(t)$  taken with respect to the trajectory, one takes variations  $\delta t_i$  with respect to the impact time<sup>1</sup>. For brevity, we exclude the variational arguments here, but the principle's resulting stationarity conditions imply that for all  $t \in [0, T] \setminus \{t_i\}$  the system evolves on  $C$  according to the standard Euler-Lagrange equations

$$\frac{d}{dt} \left( \frac{\partial L}{\partial \dot{q}} \right) - \frac{\partial L}{\partial q} = 0. \quad (2)$$

Furthermore, stationarity indicates that at  $t = t_i$  the system must satisfy the following impact conditions

$$P^T(q_i) \left[ \frac{\partial L}{\partial \dot{q}} \right]_{t_i^-}^{t_i^+} = 0, \quad (3)$$

$$E|_{t_i^-}^{t_i^+} = 0, \quad (4)$$

where  $q_i = q(t_i^-) = q(t_i^+)$  is the system's configuration at impact,  $E : TQ \rightarrow \mathbb{R}$  is the system's energy defined as  $E(q, \dot{q}) = \dot{q}^T \frac{\partial L}{\partial \dot{q}} - L$ , and  $P(q) : \mathbb{R}^{n-1} \rightarrow T_q \partial C$  is a null space matrix [12] with the property

$$\text{range}(P(q)) = \text{null}(\nabla \phi(q)) = T_q \partial C.$$

The premultiplication by  $P^T(q)$  that appears in (3) serves to project that equation's momentum balance onto the space  $T^* \partial C$ . Essentially, the impact equations (3) and (4) indicate a conservation of momentum tangent to  $\partial C$  and a conservation of energy  $E$  across the impact. Notice that the variational principle makes no explicit indication about the behavior of the system's momentum normal to  $\partial C$ .

It may be helpful to view (3) in terms of the equivalent condition

$$\left[ \frac{\partial L}{\partial \dot{q}} \right]_{t_i^-}^{t_i^+} = \lambda \nabla \phi(q_i), \quad (5)$$

<sup>1</sup>Formulations exist where the parameterization of time as a whole is varied, though away from the impact time  $t_i$  this only serves to generate redundant stationarity conditions.

where  $\lambda$  is a Lagrange multiplier dictating the magnitude of an impulse to the system in the direction  $\nabla \phi(q_i)$ . This equation is one dimension larger than that of (3), but provides an expression on  $T^*C$  describing the impact mechanics.

In robotics [16], it is common to see a variety of systems (for instance, serial chain mechanisms) modeled with Lagrangians of the form

$$L(q, \dot{q}) = \frac{1}{2} \dot{q}^T M(q) \dot{q} - V(q), \quad (6)$$

where  $M(q)$  is a symmetric positive definite mass matrix and  $V(q)$  is a potential function. For this Lagrangian, we have  $\frac{\partial L}{\partial \dot{q}} = M(q) \dot{q}$  and

$$E(q, \dot{q}) = \frac{1}{2} \dot{q}^T M(q) \dot{q} + V(q).$$

If we assume  $M(q)$  is invertible on all of  $\partial C$ , then the system of equations (5) and (4) yields the explicit solution<sup>2</sup>

$$\lambda = -2 (\nabla \phi^T M^{-1} \nabla \phi)^{-1} \nabla \phi^T \dot{q}(t_i^-), \quad (7)$$

$$\dot{q}(t_i^+) = \left( \mathbb{I} - 2 (\nabla \phi^T M^{-1} \nabla \phi)^{-1} M^{-1} \nabla \phi \nabla \phi^T \right) \dot{q}(t_i^-), \quad (8)$$

where all instances of  $\nabla \phi$  and  $M^{-1}$  are evaluated at  $q_i$  and  $\mathbb{I}$  signifies the  $n \times n$  identity matrix.

### B. Hamiltonian Impact Mechanics

In our coming discussion of impact simulation methods it will often be helpful to examine nonsmooth mechanics from a Hamiltonian viewpoint. Hence, we will now recast the prior subsection's results with equivalent conditions in the Hamiltonian phase space  $T^*Q$ . In order to do this, let us assume that  $L$  is hyperregular [14]. That is, the Legendre transform  $\mathbb{F}L : TQ \rightarrow T^*Q$ , defined in coordinates as

$$\mathbb{F}L : (q, \dot{q}) \mapsto (q, p) = \left( q, \frac{\partial L}{\partial \dot{q}} \right),$$

is a global isomorphism. In this case, our Lagrangian system can be extended to a Hamiltonian system on  $T^*Q$  with the Hamiltonian  $H : T^*Q \rightarrow \mathbb{R}$  defined as  $H(q, p) = E(\mathbb{F}L^{-1}(q, p))$ . Using this  $H$ , we have Hamilton's equations

$$\dot{q} = \frac{\partial H}{\partial p}, \quad (9)$$

$$\dot{p} = -\frac{\partial H}{\partial q}, \quad (10)$$

which are equivalent to (2), and the impact equations

$$p|_{t_i^-}^{t_i^+} = \lambda \nabla \phi(q_i), \quad (11)$$

$$H|_{t_i^-}^{t_i^+} = 0, \quad (12)$$

which are equivalent to equations (5) and (4).

<sup>2</sup>In actuality, (5) and (4) also admit a second solution  $\lambda = 0$ ,  $\dot{q}(t_i^-) = \dot{q}(t_i^+)$ , but we disregard this as it would cause  $q(t)$  to exit the feasible space  $C$  for  $t > t_i$ .

The Lagrangian specified in (6) is hyperregular if  $M(q)$  is invertible for all  $q \in Q$ . If that is the case, we have  $\mathbb{F}L(q, \dot{q}) = (q, M(q)\dot{q})$  and

$$H(q, p) = \frac{1}{2}p^T M^{-1}(q)p + V(q). \quad (13)$$

For this Hamiltonian system, the explicit solutions (7) and (8) are equivalent to

$$\lambda = -2(\nabla\phi^T M^{-1}\nabla\phi)^{-1}\nabla\phi^T M^{-1}p(t_i^-), \quad (14)$$

$$p(t_i^+) = \left(\mathbb{I} - 2(\nabla\phi^T M^{-1}\nabla\phi)^{-1}\nabla\phi\nabla\phi^T M^{-1}\right)p(t_i^-), \quad (15)$$

where again all instances of  $\nabla\phi$  and  $M^{-1}$  are evaluated at  $q_i$ .

### C. A Hybrid Systems Model of Impact Mechanics

The nonsmooth mechanics of the Hamiltonian system defined with (13) fit the model of a hybrid automaton [13], [1]. The automaton's state,  $(q, p)$ , evolves smoothly by (9) and (10) on a single domain,  $T^*C$ , except at any instances in time when the guard condition,  $\phi(q) = 0$ , indicates a discrete event. At those instances, the discrete reset map, defined with the combination of  $q(t_i^+) = q(t_i^-)$  and (15), is applied and evolution of the system on  $T^*C$  continues. Where applicable, we will use this automaton model of the system to describe impact simulation techniques in discrete time.

## III. STRUCTURED INTEGRATION METHODS FOR IMPACTS

We now consider the task of numerically integrating the nonsmooth mechanics presented in Section II. In all of our efforts, we fundamentally rely on discrete mechanics and VI theory [14], [7]. For smooth dynamics, VIs represent a class of symplectic-momentum integration schemes that exhibit stable energy behavior. In the nonsmooth setting, we will compare our original impact integration method (IIM) with two existing methods. The three follow the same general structure for identifying and resolving impacts, but differ in their respective discretization of the impact equation (12). Where possible, we analyze the methods analytically; however, much of their evaluation is reserved for the following section containing numerical results.

### A. Integrating Smooth Dynamics

Discrete mechanics specifies that in order to capture smooth dynamics in discrete time we begin by replacing our notion of the state space  $TQ$  with  $Q \times Q$  and substitute for the continuous trajectory  $q(t)$  a discrete path  $q_d : \{0, h, 2h, \dots, Nh = T\} \rightarrow Q$ ,  $N \in \mathbb{N}$ . This path is defined such that  $q_k := q_d(kh)$  is considered an approximation to  $q(kh)$ . Based on these discretizations, the action integral in Hamilton's principle (1) is approximated on a time slice  $[kh, (k+1)h]$  using a discrete Lagrangian  $L_d : Q \times Q \times \mathbb{R}$ . For instance, in our numerical simulations to come we make

use of the Störmer-Verlet [6] producing discrete Lagrangian

$$L_d(q_k, q_{k+1}, h) := \frac{h}{2} \left( L \left( q_k, \frac{q_{k+1} - q_k}{h} \right) + L \left( q_{k+1}, \frac{q_{k+1} - q_k}{h} \right) \right), \quad (16)$$

$$\approx \int_{kh}^{(k+1)h} L(q(t), \dot{q}(t)) dt.$$

Summing these approximations over the discrete path defines a discrete version of the Hamilton's principle

$$\delta \sum_{k=0}^{N-1} L_d(q_k, q_{k+1}, h) = 0, \quad (17)$$

for all variations  $\{\delta q_k\}_{k=0}^N$  with  $\delta q_0 = \delta q_N = 0$ . Stationarity in this discrete principle implies the discrete Euler-Lagrange equations

$$D_2 L_d(q_{k-1}, q_k, h) + D_1 L_d(q_k, q_{k+1}, h) = 0, \quad (18)$$

for all  $k \in \{1, \dots, N-1\}$ , where the notation  $D_i$  indicates differentiation with respect to the  $i^{\text{th}}$  argument. For integration purposes, (18) constitutes an implicit map from  $(q_{k-1}, q_k)$  to  $q_{k+1}$ .

VIs can also be viewed in the Hamiltonian setting. Following the definitions of [14], consider discrete Legendre transforms  $\mathbb{F}^+ L_d, \mathbb{F}^- L_d : Q \times Q \times \mathbb{R} \rightarrow T^*Q$  defined in coordinates as

$$\mathbb{F}^+ L_d : (q_0, q_1, h) \mapsto (q_1, p_1) = (q_1, D_2 L_d(q_0, q_1, h)),$$

$$\mathbb{F}^- L_d : (q_0, q_1, h) \mapsto (q_0, p_0) = (q_0, -D_1 L_d(q_0, q_1, h)).$$

Using these definitions, the discrete equations of motion (18) can be rewritten

$$\mathbb{F}^+ L_d(q_{k-1}, q_k, h) = \mathbb{F}^- L_d : (q_k, q_{k+1}, h).$$

In practice, when integrating in the Hamiltonian setting one starts at a given  $(q_k, p_k)$ , first solves  $p_k = -D_1 L_d(q_k, q_{k+1}, h)$  for the unknown  $q_{k+1}$ , and finally explicitly calculates  $p_{k+1} = D_2 L_d(q_k, q_{k+1}, h)$ . This process defines a discrete numerical flow  $\Phi_h : T^*Q \rightarrow T^*Q$  satisfying  $\Phi_h(q_k, p_k) = (q_{k+1}, p_{k+1})$ . It should come as no surprise that the uniqueness of this flow (both forwards and backwards in time) hinges on the regularity of the discrete Lagrangian  $L_d$ .

VI methods do not exactly conserve energy but do, as stated prior, exhibit stable energy behavior. The guarantee of this stability can be demonstrated via backwards error analysis, which shows that the discrete flow  $\Phi_h$  for any VI method provides the exact solution to a modified differential equation which is also Hamiltonian [7]. This implies that every VI method has associated with it a modified Hamiltonian (MH) as a conserved quantity. Furthermore, it is true in general that the MH differs from that of the system being simulated by  $O(h^p)$  where  $p$  is the order of the VI in use [6]. Often the analytical expression for the MH is an infinite series, but one can still gain insight when working with truncated expressions. For instance, following the process outlined in

[7] we have calculated as an  $O(h^3)$  truncation of the MH for the Störmer-Verlet VI the expression<sup>3</sup>

$$\tilde{H} = H + \frac{h^2}{24} (2H_{qq}(H_p, H_p) + 2H_{qp}(H_p, H_q) - H_{pp}(H_q, H_q)),$$

where  $H_q$  and  $H_p$  are partial derivatives of the Hamiltonian  $H$ , and  $H_{qq}$ ,  $H_{qp}$ , and  $H_{pp}$  are second derivatives of  $H$  that act as bilinear mappings. For high dimensional mechanical systems the truncation  $\tilde{H}$  may be quite complex, however its efficient computation can be performed with the use of tree-based data structures and the `trep` simulation package [9]. The near conservation of  $\tilde{H}$  is pivotal in defining our new method for impact integration.

### B. General Structure of Impact Integration

Before examining the details of the three distinct IIMs, we first present their common structure. Each of the methods uses identical, constant timestep integration by  $\Phi_h$  until reaching a phase  $(q_j, p_j)$  that satisfies

$$\Phi_h(q_j, p_j) = (\hat{q}_{j+1}, \hat{p}_{j+1}), \quad (19)$$

$$\phi(\hat{q}_{j+1}) < 0. \quad (20)$$

Qualitatively, (19) and (20) indicate that integrating a full timestep would cause the system to leave the feasible space  $C$ , and thus an impact must occur. Rather than using  $\Phi_h$  from  $(q_j, p_j)$ , the IIMs integrate according to

$$\Phi_{\alpha h}(q_j, p_j) = (q_i, p_i^-), \quad (21)$$

$$\phi(q_i) = 0, \quad (22)$$

where a partial timestepping constant,  $\alpha \in [0, 1]$ , has been introduced. Inclusion of  $\alpha$  in (21) allows one to resolve the impact configuration,  $q_i \in \partial C$ , as well as the pre-impact momentum,  $p_i^-$ , at a nonuniform time,  $t_i = (j + \alpha)h$ . With (21) and (22) solved, the methods enforce

$$p_i^+ = p_i^- + \lambda \nabla \phi(q_i), \quad (23)$$

which is essentially the impact law specified by (11). Notice that without the condition (12) or some substitute for it, the system (23) is underdetermined in the variables  $(\lambda, p_i^+)$ . The IIMs examined in the subsections that follow each complete this set of equations in a distinct manner. We lastly note that each IIM, regardless of how (23) is solved, uses partial timestepping in the form

$$\Phi_{(1-\alpha)h}(q_i, p_i^+) = (q_{j+1}, p_{j+1}), \quad (24)$$

to return to the same uniform mesh of time on which the system was evolving prior to impact. Following this, integration with  $\Phi_h$  resumes until the next impact is detected.

<sup>3</sup>This expression agrees with the calculations in [6] up to a sign. We believe their expression (pp. 422) should have a negative before  $\frac{1}{24} \nabla U(q)^T \nabla U(q)$ .

### C. Discrete Time Energy Conservation (DTEC)

The first IIM that we consider is precisely that derived in [5]. As the method conserves a discrete time definition of energy through the impact, we refer to it as the DTEC method. The distinct feature of this method, relative to the others we will discuss, is its use of  $-D_3L_d : Q \times Q \times \mathbb{R}$  to define a conservation law for impacts in discrete time. This is not a conserved quantity during smooth simulations and, as we will see in simulations to come, its conservation at isolated instances in time cannot provide any overall structured energy behavior.

The derivation of this method in [5] relies on an adaptation of the discrete Hamilton's principle (17) to approximate non-smooth trajectories like those considered by the continuous time principle (1). By grounding the method in a discrete Hamilton's principle, it does inherit an elegant discrete symplectic structure (in fact it's the only fully symplectic method of the three we consider). The derivation is done in the Lagrangian setting, so it produces impact conditions expressed on the discrete tangent space  $Q \times Q$ . Concretely, the discrete variational principle produces as a stationarity condition

$$-D_3L_d(q_j, q_i, \alpha h) = -D_3L_d(q_i, q_{j+1}, (1 - \alpha)h), \quad (25)$$

as well as Lagrangian equivalents of equations (21), (23), and (24).

For one unfamiliar with VIs, it may not be clear how (25) represents a discretization of (12), or more appropriately (4) (since the method operates in the Lagrangian setting). In fact, it is an extended (meaning space-time) discrete Lagrangian structure [14] that causes  $-D_3L_d : Q \times Q \times \mathbb{R}$  to represent a discretization of the continuous time  $E$ . We cannot illustrate the entire theory here, but consider that for  $L$  as in (6) and  $L_d$  as in (16) we have the expression

$$-D_3L_d(q_0, q_1, h) = \frac{1}{2} \frac{(q_1 - q_0)^T}{h} \left( \frac{M(q_0) + M(q_1)}{2} \right) \frac{q_1 - q_0}{h} + \frac{V(q_0) + V(q_1)}{2},$$

which clearly approximates the continuous time energy  $E(q(\frac{h}{2}), \dot{q}(\frac{h}{2}))$ . This points, perhaps, to a shortcoming of the method. If  $-D_3L_d$  approximates the system's energy in the middle of timesteps, then condition (25) equates approximations of the energy at  $t = (j + \frac{\alpha}{2})h$  and  $t = (j + \frac{1+\alpha}{2})h$  (instead of the precise pre- and post-impact times). If  $-D_3L_d$  was a conserved quantity of the discrete flow  $\Phi_h$ , there might be reason to enforce this equality. However, this is not the case, and in requiring this condition the DTEC impact law actually ignores the existing MH conservation law for  $\Phi_h$ .

As an analytical illustration of potential shortcomings in the DTEC method, we present the following example. Consider a simple point mass on the real line in a linear potential field, meaning  $Q = \mathbb{R}$  and  $L = \frac{1}{2}\dot{q}^2 - q$ . We will subject this mass to the unilateral constraint  $\phi(q) = q$ . Using

$L_d$  as in (16), equation (25) has the explicit solution<sup>4</sup>

$$q_{j+1} = (1 - \alpha)^2 h^2 \left( -\frac{1}{2} + \sqrt{\frac{1}{4} + \frac{-2D_3 L_d(q_j, 0, \alpha h)}{(1 - \alpha)^2 h^2}} \right).$$

Given that  $-D_3 L_d(q_j, 0, \alpha h)$  is necessarily positive, this solution grows linearly in  $h$  away from  $h = 0$ . Furthermore, it is impossible for this method to yield  $q_{j+1} < 0$  (a.k.a. multiple impacts on the interval  $[jh, (j+1)h]$ ). These facts seem contrary to the behavior we would expect given the linear potential. This example indicates that growing the timestep  $h$  doesn't just reduce the accuracy of the DTEC method, it reduces the validity of its discrete dynamics.

#### D. Continuous Time Energy Conservation (CTEC)

The second IIM we consider stems from treating the system as a hybrid automaton. As it enforces conservation of the continuous time definition of energy through the impact, we refer to it as the CTEC method. It might seem that this method's direct use of continuous time impact conditions on discrete time quantities is sensible. However this practice, like the DTEC method, ignores the underlying discrete time conservation laws provided by VIs.

Note that the general structure of integration outlined in subsection III-B treats simulation in the same manner as the hybrid system techniques provided in [2]. That is, the task is divided into sequences of continuous simulation and discrete instances of event resolution (marked by guard detection, and state reset). Although, the inclusion of partial timestepping in our simulations marks a more sensitive treatment of guard detection, which is a significant issue for hybrid system simulation [15]. In accordance with simulating the nonsmooth mechanical system as a hybrid automaton, the CTEC method resolves events (a.k.a. impacts) using conditions from the system's continuous time model. Specifically, CTEC enforces

$$H(q_i, p_i^-) = H(q_i, p_i^+), \quad (26)$$

which is just (12) applied to the discrete time entities  $q_i$ ,  $p_i^-$ , and  $p_i^+$ .

In regards to the previous subsection's point mass system, CTEC admits the explicit solution

$$q_{j+1} = (1 - \alpha) h \sqrt{2H(q_i, p_i^-)} - \frac{(1 - \alpha)^2 h^2}{2}. \quad (27)$$

The presence of the  $O(h^2)$  term indicates CTEC is capturing the dynamics governed by the linear potential force and can exhibit multiple collisions on the interval  $[jh, (j+1)h]$ . This analytical result gives support to the CTEC method, but the coming section's simulation results provide an opposing argument.

<sup>4</sup>In actuality, (25) admits two solutions for this case, but similar to our prior solution of the system (5) and (4), one is excluded as it represents the absence of a collision.

#### E. Modified Hamiltonian Conservation (MHC)

In contrast to the two prior IIMs, here we present our original technique. As it is grounded in the backward error analysis and MH conservation properties of  $\Phi_h$ , we refer to it as MHC. We draw upon the method in [3], where they apply

$$\tilde{H}(q_i, p_i^-, h) = \tilde{H}(q_i, p_i^+, h). \quad (28)$$

However, the validity of this expression depends on the discrete dynamics of  $\tilde{H}$ , meaning the accuracy to which the truncated expression is approximating the true MH (which has no dynamics). In the next section's simulation results, we will see cases in which the discrete dynamics of a given truncation  $\tilde{H}$  are nontrivial. To overcome this, and still make use of  $\tilde{H}$  to nearly conserve the MH, our MHC method utilizes additional simulation. That is, in lieu of (28), we calculate the stable values of  $\tilde{H}$  in small windows of time pre- and post-impact, and enforce equality in those values as a means of determining a solution to (23). Given prior tests and information regarding the frequency of nontrivial dynamics in  $\tilde{H}$ , one can heuristically choose the exact size of the time windows used.

In terms of the ongoing point mass example, we have no analytical notion of the the discrete dynamics of  $\tilde{H}$ . However, we can say that equations (26) and (28) are equivalent for that system. So if the dynamics of  $\tilde{H}$  are near trivial and (28) is used, the solution (27) holds for MHC as well. This is largely a function of the simplicity of the system (consider  $H_{qp}$  and  $H_{pp}$  vanish). As the following section will demonstrate, this equivalence between CTEC and MHC does not hold for systems of greater complexity.

## IV. NUMERICAL RESULTS AND COMPARISONS

In the following we compare the IIMs of section III during simulation of a double pendulum with impacts. We model the nonsmooth mechanics of this system according to the elastic impact theory of section II. We will demonstrate that the DTEC and CTEC methods perform poorly when simulating the double pendulum due to their local definitions of energy conservation. Further, we will discuss why the MHC method avoids this pitfall. The superiority of the MHC method will be presented both in terms of energy conservation and trajectory error analysis.

#### A. The Double Pendulum (DP) with Impacts

Consider a DP in the plane composed of two point masses,  $m_1$  and  $m_2$ , connected in sequence (from the origin) by inertialess rods of respective lengths  $L_1$  and  $L_2$ . We henceforth refer to the rods by their lengths. The configuration space for the DP is  $Q = \mathbb{T}^2 = S^1 \times S^1$  with coordinates  $q = (\theta_1, \theta_2)$ , where  $\theta_1$  is the angle of  $L_1$  with respect to vertical and  $\theta_2$  is the angle of  $L_2$  with respect to  $L_1$ . Under the influence of

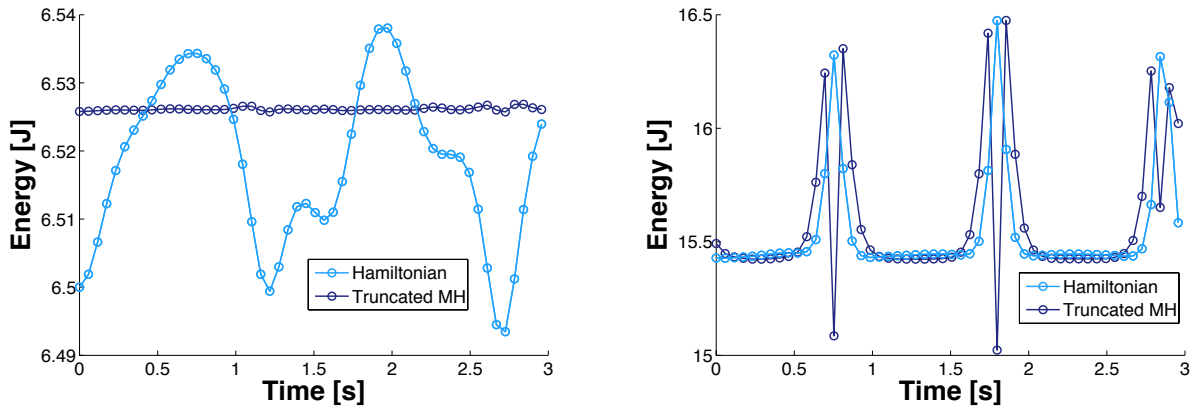


Fig. 1. Discrete time behavior of the Hamiltonian,  $H$ , and truncated MH,  $\tilde{H}$ , for two simulations of the double pendulum's smooth dynamics (no impacts). The left plot was produced using  $q_0 = [0, 0]^T$ ,  $p_0 = [8, 3]^T$  and the right with  $q_0 = [0.2, -1.5]^T$ ,  $p_0 = [3, -1.8]^T$ . Both simulations use the constant timestep  $h = 5.8 \times 10^{-2}$ . Left: Some regions of phase space produce only small scale dynamics in  $H$  and  $\tilde{H}$  during simulation, indicating only small errors relative to the conserved MH. Right: Other phase space regions produce large spikes in  $H$  and  $\tilde{H}$ . That  $\tilde{H}$  displays these spikes indicates that they stem from terms in the MH of  $O(h^4)$  or higher. To approximate the MH along trajectories that produce spikes one could make use of a truncation with higher order than  $\tilde{H}$ , or systematically identify regions away from spikes where  $\tilde{H}$  is stable.

gravity,  $g$ , the DP's Lagrangian fits the form of (6) with

$$M(q) = \begin{bmatrix} m_1 L_1^2 + m_2(L_1^2 + L_2^2 + 2L_1 L_2 c_2) & m_2(L_2^2 + L_1 L_2 c_2) \\ m_2(L_2^2 + L_1 L_2 c_2) & m_2 L_2^2 \end{bmatrix},$$

$$V(q) = m_1 g L_1 (1 - c_2) + m_2 g (L_1 (1 - c_2) + L_2 (1 - c_{12})),$$

where we've introduced the shorthand  $c_i = \cos \theta_i$  and  $c_{ij} = \cos(\theta_i + \theta_j)$ . We note that

$$\det(M(q)) = m_2 L_1^2 L_2^2 (m_1 + m_2 (1 - c_2^2)),$$

which never vanishes on  $Q$  for positive  $m_1$  and  $m_2$ . Thus the DP's Lagrangian is in fact hyperregular.

When introducing impacts into the system, we apply the unilateral constraint

$$\phi(q) = L_1 s_1 + L_2 s_{12} + 0.25,$$

where  $s_i = \sin \theta_i$  and  $s_{ij} = \sin(\theta_i + \theta_j)$ . Physically, this constrains the horizontal position of  $m_2$  (the end of the DP) to values greater than or equal to  $-0.25$ .

### B. Smooth Integration Results

Prior to simulating the DP's nonsmooth mechanics, we performed simulations in the absence of impacts for a variety of initial conditions in the phase space. In all simulations we used parameters  $m_1 = m_2 = L_1 = L_2 = 1$  and  $g = 10$ , and integrated according to the discrete flow  $\Phi_h$  as defined with (16). Results regarding the discrete time behavior of the Hamiltonian,  $H$ , and the truncated MH,  $\tilde{H}$ , during two specific simulations are presented in Figure 1. These two simulations are representative of our entire sampling of the phase space. Some initial conditions, such as those used for the left plot, produced trajectories with relatively small variation in  $H$  and almost no variation in  $\tilde{H}$  (as evidence of accurate approximation of the true MH). However, initial conditions such as those used for the right plot produced

trajectories where low variation in  $H$  was regularly interrupted by brief but large spiking deviations. As  $\Phi_h$  exactly conserves the MH, these deviations indicate that the error between  $H$  and the MH can vary significantly in different regions of the phase space. Additionally, we found that  $\tilde{H}$  exhibited similar spiking deviations, meaning we can attribute the cause of the spikes to terms in the true MH of  $O(h^4)$  or higher.

The observation that our  $O(h^3)$  approximation of the MH may still exhibit nontrivial dynamics stresses the importance of our MHC method. Essentially, if one was to naively solve the system (23) and (28) in a region of phase space where  $\tilde{H}$  greatly differs from the MH, the solution could produce an undesired change in the value of the MH. By conserving the stable value of  $\tilde{H}$  before and after impact, our MHC method avoids this potential for energy drift. An alternative to this method could be to calculate a higher order approximation  $\tilde{\tilde{H}}$  and still use (28), though who knows what order, if any, could eliminate the spiking behavior.

### C. Impact Integration Results

As means of comparing IIMs, we simulated the DP with impacts using each method with common initial conditions and a variety of timesteps. Results for each method in terms of the discrete behavior of  $H$  and the error of trajectories relative to a benchmark simulation are shown in Figure 2. Given our knowledge of the spiking deviations in  $H$ , the left plot shows an expected result. The DTEC and CTEC methods, in relying on local expressions of the DP's energy in discrete time, incur significant errors when an impact occurs during a spike in  $H$ . By using the modifications discussed in the previous subsection, the MHC method is not misled by similar spikes in  $\tilde{H}$ ; the plot indicates that preservation of stable values of  $\tilde{H}$  leads to good behavior in  $H$ . We should also note, it does not seem possible to modify DTEC or CTEC to conserve stable values in the same manner

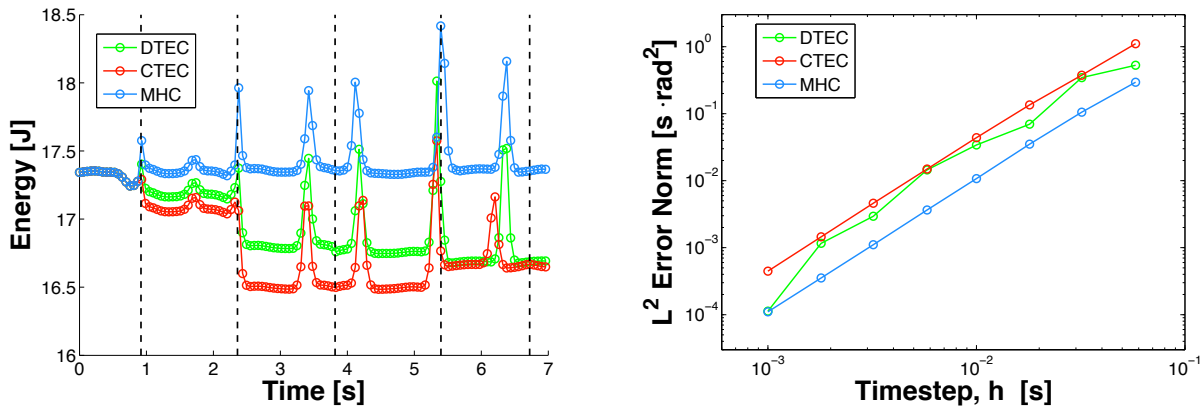


Fig. 2. Left: Discrete time behavior of the Hamiltonian,  $H$ , for simulations of the double pendulum with impacts using each of the IIMs at a timestep of  $h = 5.8 \times 10^{-2}$ . The trajectory's five impact times (from the CTEC simulation) are indicated by black dashed lines. The first, second and fourth impacts occur when there are significant higher order terms in the MH, as indicated by spiking behavior in  $H$ . As a result, they cause undesirable drift in DTEC and CTEC results. Right: A comparison of the  $L^2$  convergence of simulation trajectories to a benchmark simulation. MHC displays the best accuracy and consistent order of the method across the full range of timesteps. All simulations use  $q_0 = [0.5647, 1.1106]^T$  and  $p_0 = [3.7270, 0.2415]^T$ .

as MHC. The primary reason for this is an overall lack of stability in  $-D_3L_d$  and  $H$  along trajectories. Imagine trying to determine the correct value of  $H$  to conserve from the interval between the first and second collision, where there is little to no stable behavior in  $H$ .

The plot in the right half of Figure 2 shows, for each IIM, convergence in  $L^2$  norm of the error between simulated trajectories and a benchmark simulation produced with the CTEC method<sup>5</sup> at a timestep of  $h = 10^{-4}$ . This plot demonstrates some additional benefits of MHC relative to DTEC and CTEC. Foremost, MHC is the most accurate of the three methods across the full range of timesteps used, consistently beating the (least accurate) CTEC method by a factor of four in the error norm. Also, MHC displays very consistent second order accuracy across the full range of timesteps, especially relative to the erratic curve provided by the DTEC method<sup>6</sup>. Consistent second order convergence indicates that MHC would perform well in automated time step selection schemes [8].

## V. CONCLUSIONS AND FUTURE WORKS

### A. Conclusions

The MHC method extends the inherently stable energy behavior of VIs to systems undergoing elastic impacts. MHC identifies the appropriate quantity, the stable value of  $\tilde{H}$ , to conserve in simulation. In conserving this quantity through impacts, rather than the local expressions of the system's energy used by the existing DTEC and CTEC methods, MHC remains true to the backwards error analysis for VIs. By preserving this structure MHC provides desirable results that

<sup>5</sup>While error calculations were performed relative to the CTEC method's benchmark, in actuality simulations at  $h = 10^{-4}$  were performed with all three IIMs. Given the  $L^2$  norm of the error between benchmarks is  $O(10^{-6})$ , the choice of benchmark method does not influence the given plot.

<sup>6</sup>The convergence of DTEC here directly conflicts with the analysis provided in [5]. Their results likely show better convergence due to using a short time horizon (one impact) and a separable example system (that is, a system with  $H(q, p) = T(p) + V(q)$ , which the DP is not).

are superior to the DTEC and CTEC methods in terms of the stability of  $H$  in discrete time, the accuracy of simulation trajectories at a given timestep, and the consistent order of accuracy of the method.

### B. Future Works

The encouraging results we have presented regarding MHC provide motivation for a number of future developments for the method. Foremost, though it was not noticeable in our simulation results, the partial timestepping defined by (21) and (24) necessarily introduces drift in the MH. To fully complete the theory for our backwards error analysis approach, these conditions must be replaced with mappings that conserve the MH. This will involve deriving an alternate discrete flow, differing from  $\Phi_h$ , to apply on these partial timesteps.

The comparison we have made between IIMs made use of a trajectory known to expose weaknesses in the DTEC and CTEC methods. Under different initial conditions, the performance difference between methods may be more or less drastic. Using further simulation, we intend to characterize the difference between methods as a function of initial conditions. This will likely establish the dominance of MHC over DTEC and CTEC in an average sense.

The addition of forcing and control in MHC simulations is an obvious next step. If smooth mechanics are any indication [14], a reliable structured representation of the conservative case is the appropriate first step to producing simulations that accurately capture forcing and dissipation. With the inclusion of generalized forces MHC can naturally be extended, in the same manner as many other VIs, into an optimal control generation scheme using DMOC [10].

## VI. ACKNOWLEDGMENTS

This material is based upon work supported by the National Science Foundation under award CCF-0907869. Any opinions, findings, and conclusions or recommendations expressed in this material are those of the author(s) and

do not necessarily reflect the views of the National Science Foundation.

#### REFERENCES

- [1] R. Alur, C. Courcoubetis, T. A. Henzinger, and P. H. Ho, "Hybrid automata: An algorithmic approach to the specification and verification of hybrid systems", in *Hybrid Systems*. New York: Springer-Verlag, 1993, vol. 736, Lecture Notes in Computer Science, pp. 209–229.
- [2] M. Anderson, *Object-Oriented Modeling and Simulation of Hybrid Systems*, PhD thesis, Lund Institute of Technology, Dec. 1994.
- [3] S. D. Bond and B. J. Leimkuhler, "Stabilized Integration of Hamiltonian Systems with Hard-Sphere Inequality Constraints," *SIAM Journal Sci. Comput.*, vol. 30 (1), pp. 134–147, 2007.
- [4] B. Brogliato, *Nonsmooth Mechanics*. New York: Springer-Verlag, 1998.
- [5] R. Fetecau, J. E. Marsden, M. Ortiz, and M. West, "Nonsmooth Lagrangian Mechanics and Variational Collision Integrators," *SIAM Journal on dynamical systems*, vol. 2, 2003, pp.381–416.
- [6] E. Hairer, C. Lubich and G. Wanner, "Geometric numerical integration illustrated by the Störmer-Verlet method," *Acta Numerica*, vol. 12, 2003, pp. 399–450.
- [7] E. Hairer, C. Lubich, and G. Wanner, *Geometric Numerical Integration: Structure-Preserving Algorithms for Ordinary Differential Equations*. New York: Springer, 2002.
- [8] E. Hairer, S. P. Norsett, and G. Wanner, *Solving Ordinary Differential Equations I: Nonstiff Problems*, New York: Springer Verlag, 1993.
- [9] E. Johnson and T. D. Murphey, "Scalable variational integrators for constrained mechanical systems in generalized coordinates," *IEEE Trans. on Robotics*, 25(6), pp. 1249–1261, 2009.
- [10] O. Junge, J. E. Marsden, and S. Ober-Blöbaum, "Discrete Mechanics and Optimal Control," in *Proceedings of the 16th IFAC World Congress*, Prague, 2005.
- [11] V. V. Kozlov and D. V. Treshchev, *Biliards: A Genetic Introduction to the Dynamics of Systems with Impacts*. Providence, RI: Amer. Math. Soc., 1991.
- [12] S. Leyendecker, J. E. Marsden, and M. Ortiz, "Variational integrators for constrained dynamical systems," *ZAMM*, vol. 88, 2008, pp. 677 – 708.
- [13] J. Lygeros, K. Johansson, S. Simic, J. Zhang, and S. S. Sastry, "Dynamical properties of hybrid automata," *IEEE Trans. Autom. Control*, vol. 48, 2003, pp. 2–17.
- [14] J. E. Marsden and M. West, "Discrete mechanics and variational integrators," *Acta Numerica*, vol. 10, 2001, pp. 357–514.
- [15] P. J. Mosterman, "An Overview of Hybrid Simulation Phenomena and Their Support by Simulation Packages," in *Proceedings of the Second International Workshop on Hybrid Systems: Computation and Control*, p.165-177, March 29-31, 1999.
- [16] R. M. Murray, Z. Li, and S. S. Sastry, *A Mathematical Introduction to Robotic Manipulation*. Boca Raton, FL: CRC, 1994.
- [17] D. Pekarek, *Variational Methods for Control and Design of Bipedal Robot Models*, PhD thesis, California Institute of Technology, Jun. 2010.
- [18] D. Pekarek and J. E. Marsden, "Variational Collision Integrators and Optimal Control, in *Proceedings of the 18th International Symposium on Mathematical Theory of Networks and Systems*, Blacksburg, VA, 2008.
- [19] L. C. Young, *Lectures on the Calculus of Variations and Optimal Control Theory*, W. B. Saunders Company, Philadelphia, 1969, corrected printing, Chelsea, UK, 1980.